Patterns of Local Circulation in the Itaipu Lake Area: Numerical Simulations of Lake Breeze

SÔNIA M. S. STIVARI

Department of Physics, State University of Maringá, Maringá, Brazil

AMAURI P. DE OLIVEIRA, HUGO A. KARAM, AND JACYRA SOARES

Group of Micrometeorology, Department of Atmospheric Sciences, IAG-USP, São Paulo, Brazil

(Manuscript received 31 October 2001, in final form 12 June 2002)

ABSTRACT

The lake-breeze circulation in the Itaipu region was investigated numerically using a nonhydrostatic version of the Topographic Vorticity Model. The area of study corresponds to a 100 km × 180 km rectangle, located on the Brazil–Paraguay border, with Itaipu Lake in its center. The characteristics of the lake breeze generated by the numerical experiments were consistent with the observations available in the area. The numerical experiments have shown that the land use effect is important in the spatial distribution of the lake-breeze circulation and that the topography contributes to modulating the breeze intensity, with the daytime valley–mountain circulation intensifying the lake breeze. However, the circulation pattern observed during daytime over the region is mainly due to the Itaipu Lake presence. The numerical results indicated that Itaipu Lake is able to generate and sustain a lake breeze, with 3.5 m s^{-1} of maximum intensity and 1500-m depth, that propagates inland at 5.1 km h^{-1} under typical undisturbed and calm-wind summer conditions.

1. Introduction

Itaipu Lake was formed in 1982 as part of the water reservoir of the Brazilian–Paraguay Itaipu hydroelectric power plant (Fig. 1). With power of 12 600 MW, this plant provides 79 billion KW h yr^{-1} to Brazil and Paraguay. The formation of this lake has altered considerably the geographic features of the Brazil–Paraguay border region. The largest horizontal extension of the lake—170 km—is aligned in the north–south direction. In the east–west direction the lake extends 7.5 km. On the eastern side (Brazil), most of the area around the lake is used for agricultural activities, while on the western side (Paraguay) there is considerably more land covered by forest.

The analyses of the meteorological data available on this region indicated that the lake-breeze circulation is a dominant feature in the Itaipu Lake local climate (Stivari 1999). These observations do not have the temporal and spatial resolution to undoubtedly sustain the lake-breeze hypothesis. Therefore, it is not possible to discard the role played by mountain–valley circulation (Fig. 2a) and/or by small-scale circulation induced by the land use (Fig. 2b) on the circulation observed in the Itaipu Lake area. The topography could induce circulations similar to the lake-breeze circulation. For instance, mountain–valley circulation (as well as lake-breeze circulation) could generate a systematic subsidence over the valley during daytime, inhibiting the cloud formation and, therefore, reducing the precipitation in the vicinity of Itaipu Lake (Pielke and Segal 1986; Durran 1990). Because the mountain–valley circulation is expected to be in phase with the lake-breeze circulation, the local circulation could be reinforced in the lake's wider regions when both effects are presented. The impact caused by the coupled circulation would be stronger in the local climate. The role played by the land use–induced circulations on the lake-breeze and topographic circulations are difficult to foresee (Segal et al. 1997). For instance, areas occupied by tall vegetation could restrain the flow and inhibit the lake-breeze and mountain–valley circulations (which seems to be the case on the western side of Itaipu Lake; Fig. 2b). On the other hand, the thermal contrast between vegetated and nonvegetated areas could reinforce these circulations (which seems to be the case on the eastern side of Itaipu Lake; Fig. 2b).

Corresponding author address: Amauri Pereira de Oliveira, Department of Atmospheric Sciences, IAG-USP, Rua do Matão 1226, 05508-900, São Paulo, SP, Brazil.
E-mail: apdolive@usp.br

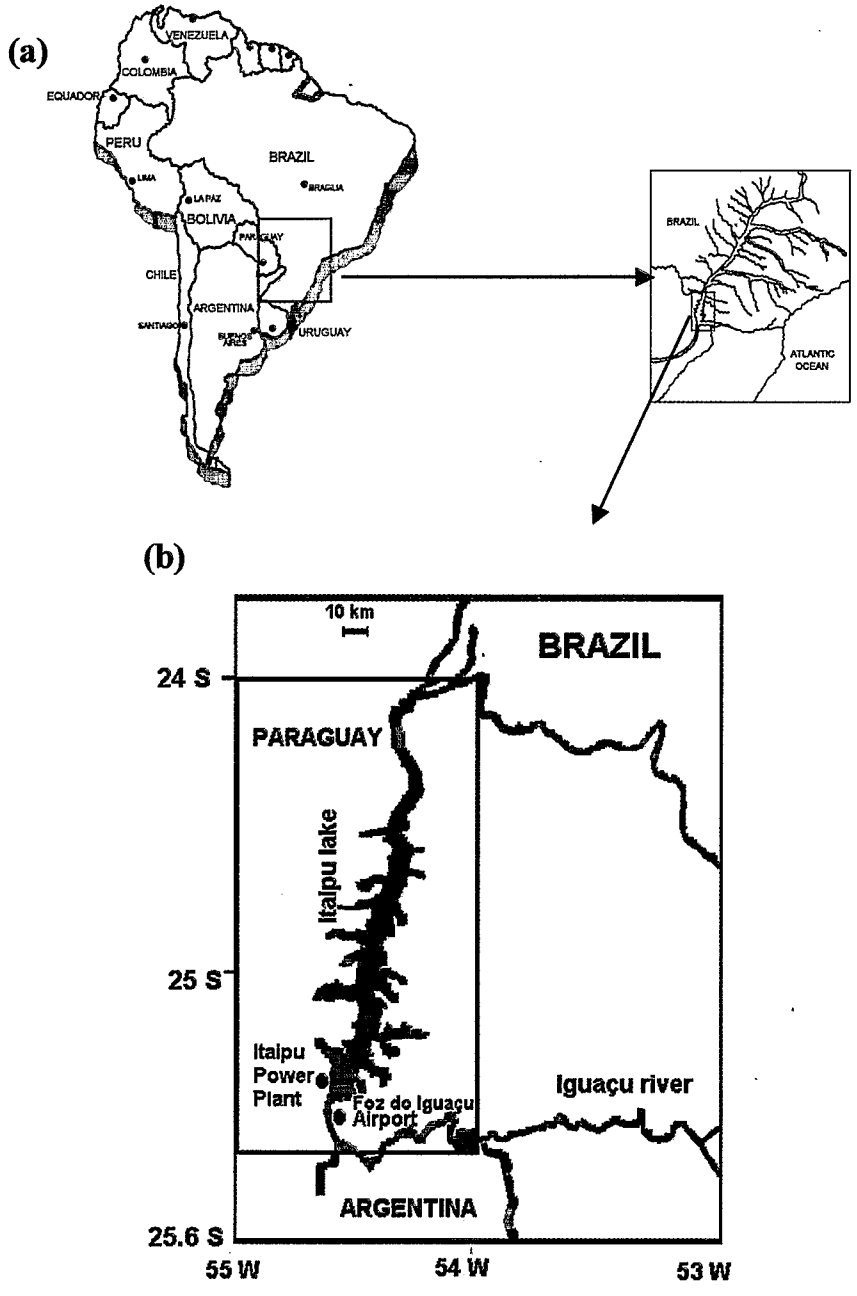

FIG. 1. Geographic maps indicating the Lake Itaipu region. The rectangle covers the lake area. The meteorological stations at Foz do Iguaçu Airport (Brazil) and the Itaipu power plant (Paraguay) are indicated by solid circles.

This work investigates, using a mesoscale numerical model (Schayes and Thunis 1990; Schayes et al. 1996), the role played by topography, land use, and Itaipu Lake on the observed circulation patterns. The utilized model is a nonhydrostatic (NH) version of the Topographic Vorticity Model (TVM) developed by Thunis and Clappier (2000).

The main objective of this work is to address, numerically, the following questions:

1) Can the Itaipu Lake generate and sustain a lake-breeze circulation?
2) How do topography and land use contribute to the lake-breeze circulation?
3) What are the characteristics of the lake-breeze circulation in the Itaipu area?
4) What is the impact of the lake-breeze circulation on the local planetary boundary layer (PBL)?

The numerical model used here was originally de-

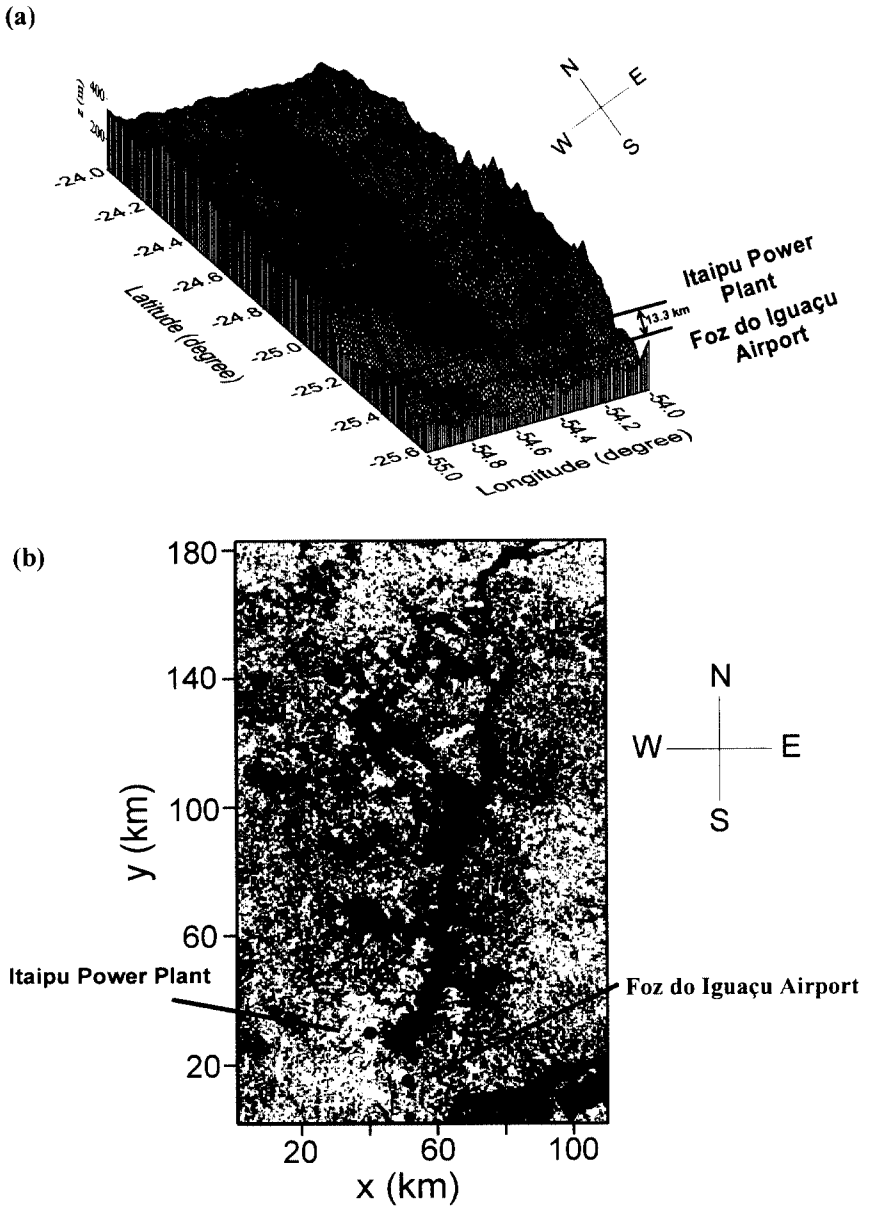

FIG. 2. (a) Topography of the Itaipu Lake region. The lake is located in the central portion of the valley. The horizontal lines indicate the latitudes of the Itaipu power plant (25°24′S, 54°36′W) and Foz do Iguaçu Airport (25°35′S, 54°29′W). (b) Land use distribution corresponding to the satellite image obtained on 21 Oct 1995. This area presents four dominant classes of surface occupation: lake and river (blue), forest (green), pasture (yellow), and agricultural (red) areas. The solid circles indicate the Itaipu power plant and Foz do Iguaçu Airport locations.

veloped as a two-dimensional and hydrostatic mesoscale model (Bornstein 1975). This first version, called URBMET, was used to simulate the planetary boundary layer structure over urban areas located in flat terrain. Subsequently, URBMET was expanded to three dimensions to simulate interactions between urban canopy and synoptic-scale systems in New York City, New York. The URBMET computational structure was maintained and the topographic effects were incorporated using the vorticity equations in the sigma-Z coordinate system. This version, called TVM, was developed by Schayes and Thunis (1990) and was classified as a mesoscale-β model (Bornstein et al. 1996; Schayes et al. 1996).

More recently, Thunis and Clappier (2000) developed the nonhydrostatic version of TVM (NH-TVM). This version—used here—is based on the numerical solution of the horizontal components of the vorticity equation and applies the gauge transformation to recover the zonal and meridional wind component field. The NH-TVM

was successfully used to simulate the local circulation in the Iberian Peninsula (Martin et al. 2001a,b).

2. Site and observations

Itaipu Lake is located in the central portion of the Paraná River valley, in the south of Brazil, near the Brazil–Paraguay border within the following geographic limits: 24°05′–25°33′S and 54°37′–54°00′W. The lake is 170 km long and approximately 7.5 km wide (Fig. 1). The investigated region is characterized by complex topography and land use. The topography, indicated in Fig. 2a, was obtained from the Instituto Brasileiro de Geografia e Estatistica (IBGE) 1:500 000-km topographic chart, and the positions of the major geographic features (lakes, rivers, etc.) were confirmed by the global topographic GTOPO30 dataset. The lake is located in a 300–400-m-deep valley.

The land use distribution employed here was based on the Landsat thematic mapper (TM) image from 21 October 1994 (Stivari 1999). It is composed of four dominant classes: forest (~28%), water (~8%), pasture (~34%), and agricultural (~30%) areas, indicated in Fig. 2b by green, blue, yellow, and red, respectively. Except for the latter area, which has a seasonal pattern related to different crops, all the other areas have not suffered significant modifications since the lake formation in 1984.

The observational evidence of the lake breeze in Itaipu Lake is based on conventional meteorological data gathered from two meteorological surface stations (Stivari 1999). The geographical locations of the stations can be seen in Fig. 2b: Foz do Iguaçu Airport (25°35′S, 54°29′W) and the Itaipu power plant (25°24′S, 54°36′W). These stations are 13.3 km apart (Fig. 2a), in the longitudinal (N–S) direction. These stations are located, respectively, on the Brazilian and Paraguayan sides of Itaipu Lake at 220 m above mean sea level. The surface wind velocity and direction data utilized in this work correspond to the monthly averaged values observed at the Itaipu power station and Foz do Iguaçu Airport, during 1990 (January, March, April) and 1994 (October). The vertical structure of the local circulation in the Itaipu Lake area was based on radiosonde launched once a day (at 0830 LT) at Foz do Iguaçu Airport. The monthly averaged air temperature over the Itaipu power plant and the monthly averaged lake water temperature were based on daily measurements (0900, 1200, 1500, and 2100 LT) carried out between 1986 and 1994 in the vicinity of the Itaipu power plant meteorological station. The observed horizontal thermal contrast was estimated as the difference between the monthly averaged daily air temperature over Itaipu Lake and the monthly averaged daily maximum and minimum air temperature over the Itaipu power plant meteorological station. This approximation is valid because the maximum and minimum air temperatures over land occur during daytime and nighttime, respectively, and because the thermal amplitude over the lake is very small.

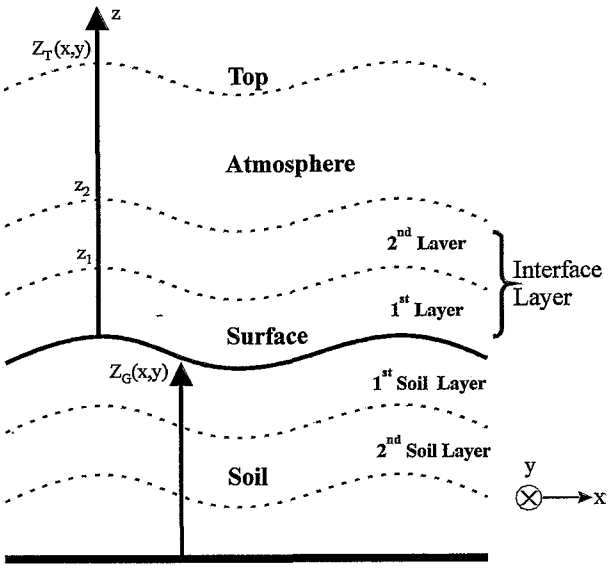

FIG. 3. Schematic representation of the vertical grid distribution in the TVM. The topography height $Z_G(x, y)$ is indicated with respect to the mean sea surface level; the vertical extent of the atmosphere $Z_T(x, y)$ is indicated with respect to the surface.

3. The TVM

A complete description of the nonhydrostatic version of the TVM can be found in Thunis and Clappier (2000). The TVM considers two atmospheric layers and two soil layers (Fig. 3). The first atmospheric layer is an interface layer, between the surface and atmosphere, in which the meteorological parameters are estimated from diagnostic relations and prognostic equations describing surface processes. The second layer represents most of the atmosphere and is located between the interface-layer top and the atmosphere top. There, all meteorological parameters are prognosticated from the equations of motion. The major characteristic of the TVM is that it uses the vorticity equation, eliminating the need to deal explicitly with the pressure. The two soil layers are basically equivalent to the vertical extent of diurnal and annual cycles of soil temperature.

The interface layer is composed of the two first vertical levels of the grid points and represents the atmospheric surface layer (Fig. 3). The first grid point (z_1) is located at the height corresponding to the roughness length (z_0). The second grid point (z_2) is located within the surface layer and defines the top of the interface-layer. The interface-layer turbulent fluxes are estimated over four types of surface: forest, agricultural, pasture, and water. The parameters used to characterize each land use are indicated in Table 1. There, the indicated soil surface temperature was used as the initial condition and the second-layer soil temperature was kept constant

TABLE 1. Surface parameters.*

Parameter	Surface type			
	Water	Forest	Agriculture	Pasture
Surface albedo	0.09	0.16	0.10	0.23
Surface emissivity	0.98	0.93	0.90	0.92
Heat capacity (10^6 J m^{-3} K^{-1})	4.18	2.0	2.0	2.0
Attenuation depth of diurnal cycle of soil temperature (m)	—	0.10	0.10	0.10
Roughness length (m)	0.001	2.000	0.100	0.020
Soil surface temperature (K)	—	299.0	299.0	299.0
Second-layer soil temperature (K)	—	300.6	300.6	300.6

* The water temperature was kept constant and equal to 302.2 K.

during simulations. The lake surface temperature was also kept constant during the numerical simulations.

Above the interface layer, the time and space evolution of thermodynamic, humidity, and dynamic structures are prognosticated from the thermodynamic, specific humidity, and vorticity equations. In this model, only the horizontal components of the vorticity equation are used. The topography (Fig. 2a) is taken into consideration by writing the equations of motion in the following topography coordinate system: (x, y, σ), where $\sigma = Z_T[(z - Z_G)/(Z_T - Z_G)]$ is the vertical coordinate, with Z_G as the topography height with respect to the mean sea level and Z_T representing the vertical extent of the atmosphere with respect to the surface (Fig. 3).

Numerical scheme, and initial and boundary conditions

The potential temperature and specific humidity at the first level of the model are initially estimated using a finite-difference scheme forward in time for the soil surface temperature and for the specific humidity equations. In this layer, the vertical turbulent fluxes and the turbulent kinetic energy are estimated analytically using Monin–Obukhov similarity theory expressions, considering the previously estimated specific humidity and potential temperature, at the second level. Above the interface layer, equations are also solved using finite-difference techniques. First, the turbulent kinetic energy (TKE) equation is solved and is used to estimate diffusion coefficients and the PBL height. This latter parameter is defined as the height at which the TKE drops to 10% of its surface value. After that, the equations are solved for potential temperature, specific humidity, and vorticity components. The components of the wind velocity are estimated from streamfunction vector components based on vorticity components.

The numerical solutions of the vorticity, thermodynamic, water vapor conservation, and TKE equations are considerably simplified using a splitting technique. Then, a third-order piecewise parabolic method (Colella and Woodward 1984) is applied to solve the advection terms in each direction. The diffusion terms are solved using the Eulerian forward scheme. The streamfunction components are numerically solved by the conjugate gradient method. All variables are allocated in a grid type "C." The horizontal domain, considered here, is 100 km in the zonal (x) direction and 180 km in the meridional (y) direction. It covers the entire valley and Itaipu Lake (Figs. 1 and 2). The grid spacings are 2 and 4 km in the x and y directions, respectively. The vertical domain extends to 13 600 m, distributed in 25 grid points. The vertical grid spacing varies from 30 m at the surface to 5200 m at the top of the atmosphere.

According to the available data, the daytime largest thermal contrast induced by Itaipu Lake occurs during the summer/autumn months. This thermal contrast is related to the larger solar energy input and the larger frequency of clear sky days occurring during this period of the year (Ratisbona 1976). The meteorological conditions were set as representative of an undisturbed summer day (yearday 344) in the region of Itaipu (Table 2). The model was initialized with a homogeneous wind from the north because this is the large-scale flow pattern expected in the Itaipu area during summer in the absence of disturbances (Ratisbona 1976). The wind intensity was chosen to be very small (2 m s^{-1}) in order to emphasize the local circulation. The vertical profiles of potential temperature and specific humidity used as initial conditions are displayed in Fig. 4.

The values of albedo, emissivity, and roughness length for each land use cover, described in Table 1, were obtained from literature considering the characteristics of the soil and vegetation in the Itaipu region, during a summer period (Sellers 1965; Stull 1988; Garratt 1992). The soil heat capacity was considered to be constant in all grid points because the soil in this region is predominantly oxisol. The surface resistance was also set constant at all grid points and its value corresponds to a condition of closed stomata. Therefore, in this region the different land use characterization is defined only in terms of roughness length, surface albedo, and emissivity. The soil temperature, used in the model, corresponds to the mean value observed in December at the Itaipu power plant meteorological station. The water temperature was based on observations carried out in Itaipu Lake.

TABLE 2. Input parameters.

Parameter	Value
Yearday	344
Latitude in the central part of the grid	25°00′S
Longitude in the central part of the grid	54°62′W
Potential temperature at the first level of the model	300 K
Specific humidity at the first level of the model	15 g kg^{-1}
Horizontal diffusion coefficient	200 m^2 s^{-1}
Initial time	0600 LT
Period of simulation	26 h
Maximum time step	30 s
Vertical grid spacing	Variable [From 30 m (surface) to 5200 m]
Zonal grid spacing	2 km
Meridional grid spacing	4 km

4. Numerical simulation results

To investigate the lake-breeze circulation, in the Itaipu area, four different numerical experiments were performed. Three of them include the lake but consider different topography and land use. The first experiment (hereinafter called expt 1) utilizes real topography and land use; in the second one, the topography is kept real but the land use is considered as agricultural over the entire land domain (expt 2). In the third experiment the topography is set flat and the land use is also set as agricultural over the entire land domain (expt 3). The last experiment considers the real topography except that the lake is removed, so the land use is regarded as agricultural over the entire domain, including the part that in reality is occupied by Itaipu Lake (expt 4). Table 3 summarizes the experiments. All the numerical simulations performed here started at 0600 LT and finished 26 h later, at 0800 LT. Therefore, the fields shown at 1500, 1800, 2100, and 0600 LT correspond, respectively, to 9, 12, 15, and 24 h of numerical simulation.

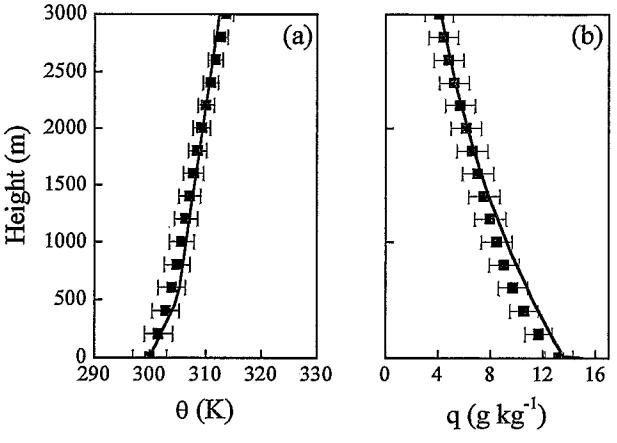

FIG. 4. Initial conditions for (a) potential temperature (K) and (b) specific humidity (g kg^{-1}) estimated from soundings carried out in Foz do Iguaçu Airport, located about 20 km southeast of Itaipu Lake (Figs. 1 and 2). The continuous line corresponds to the interpolated curve through the mean values (solid squares) and is located within the mean error (horizontal bars) range.

a. Effect of topography and land use

Figure 5 displays, for the four different experiments, the surface potential temperature and the horizontal wind field at 15 m after 12 h (1800 LT) of numerical simulation. The horizontal thermal contrast induced by Itaipu Lake, during daytime, is negative and is on the order of 7 K. The area occupied by the lake, at 1800 LT, is clearly delimited by the 306-K surface temperature contour line (Figs. 5a–5c; expts 1–3). When the lake is removed (expt 4), the thermal contrast induced by the topography at 1800 LT is smaller, on the order of 2 K (Fig. 5d). During daytime, the horizontal wind field at the second level of the model ($\sigma = 15$ m) shows a divergence area over the central portion of the Itaipu valley, exactly where the lake is located (Fig. 2b). At 1800 LT (Figs. 5a–c; expts 1–3) the lake-breeze circulation pattern is clearly noticeable in the areas around the lake. In expt 4 the divergence area is also present (Fig. 5d) but shows a much less defined spatial pattern with a smaller wind intensity when compared with the experiments with the lake. This incipient flow is associated with the mountain–valley circulation (anabatic flow). The anabatic flow is also present in the simulations with the lake and realistic topography (Figs. 5a,b) but is masked by the stronger lake-breeze circulation.

Figure 6 displays, only for expt 1, the surface potential temperature and the horizontal wind field at 15 m after 24 h (0600 LT) of numerical simulation. At nighttime, the horizontal thermal contrast induced by Itaipu Lake is positive, reaching values on the order of 10 K at the end of the night when the temperature over land reaches a minimum. For instance, at 0600 LT the area occupied by Itaipu Lake is clearly delimited by the surface temperature contour line of 299 K. During the night

TABLE 3. Numerical experiments.

Expt	Topography	Land use	Lake
1	Realistic	Realistic	Yes
2	Realistic	Agriculture	Yes
3	Flat	Agriculture	Yes
4	Realistic	Agriculture	No

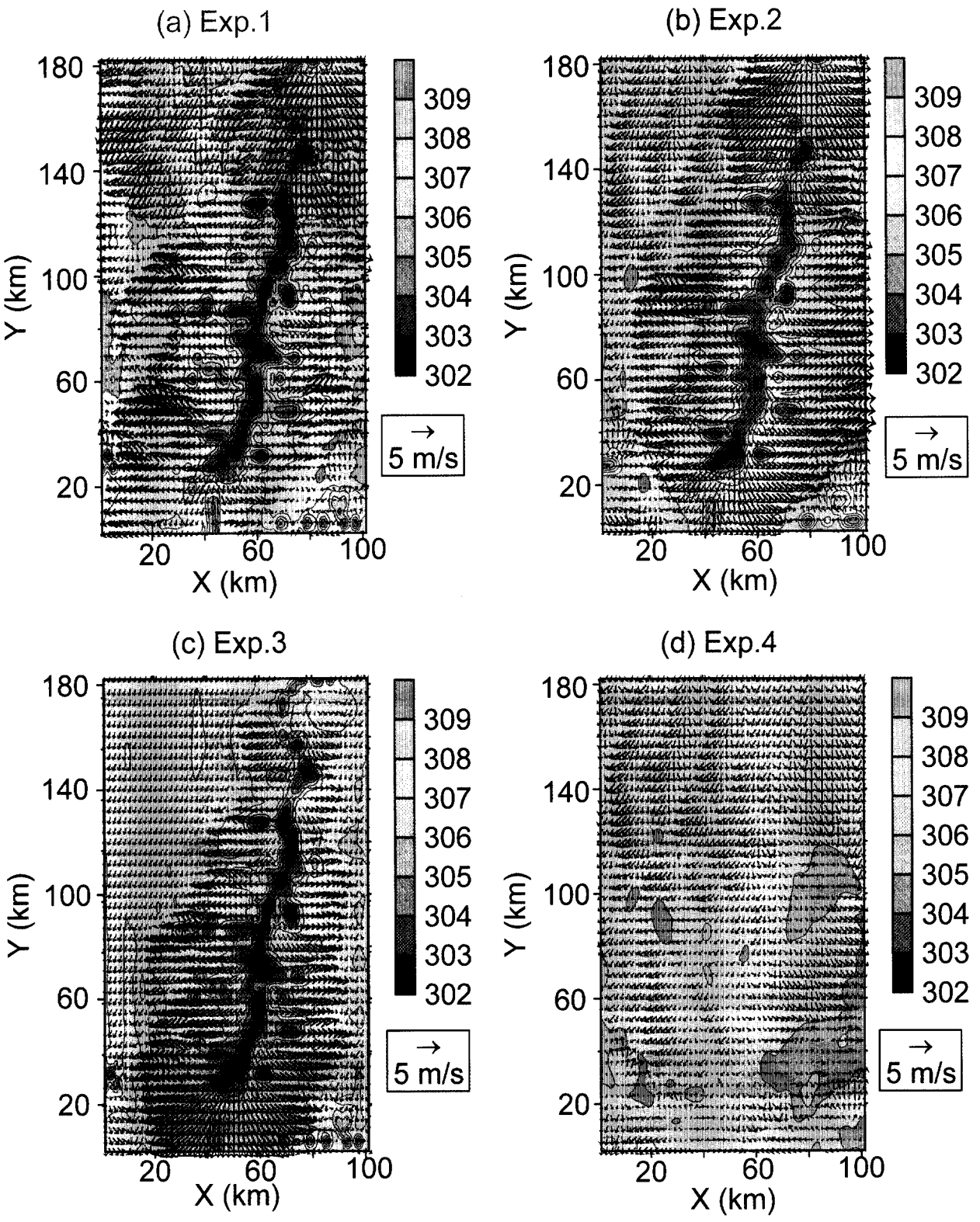

FIG. 5. Horizontal wind (m s^{-1}) at 15 m and potential temperature (K) at the surface at 1800 LT. (a) Expt 1: real topography, realistic land use, and lake presence; (b) expt 2: real topography, agricultural land use, and lake presence; (c) expt 3: level topography, agricultural land use, and lake presence; (d) expt 4: real topography, agricultural land use, and lake absence.

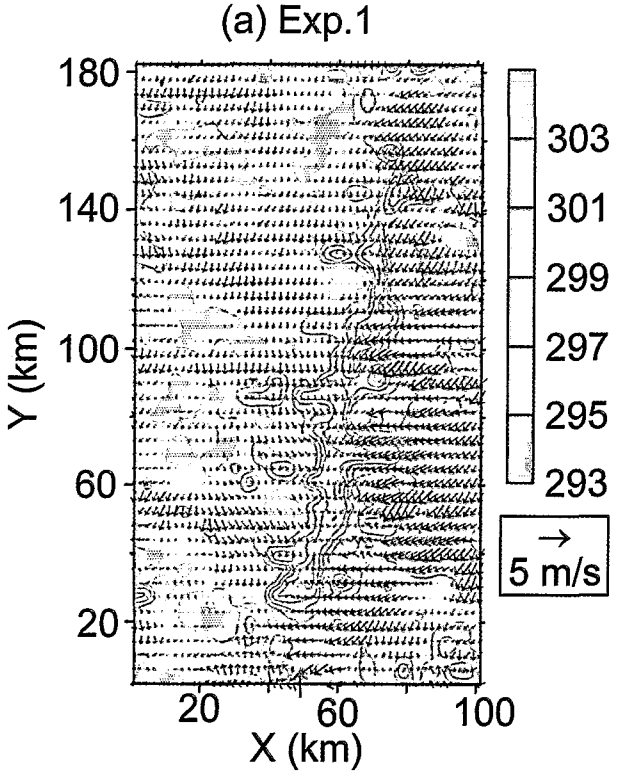

FIG. 6. Same as in Fig. 5a but at 0600 LT.

the flow close to the surface is basically laminar, and it responds to the higher (lower) topography heights, increasing (decreasing) its velocity and flowing from high to low elevations. The roughness effect can be identified comparing the wind field, at 15 m, generated by the realistic land use experiment (expt 1; Fig. 5a) with the one obtained assuming the land use is homogeneous agriculture (expt 2; Fig. 5b). In both experiments the topography is realistic and the lake is present. In expt 1, the convergence over the regions covered by forest (Fig. 2b) is noticeable, and toward the end of the daytime on the western side of Itaipu Lake, superimposed to the lake-breeze flow (Fig. 5a). Over forest the roughness length is 20 times that over agricultural areas (Table 1), slowing down the flow over forest areas. Therefore, the lake-breeze intensity is comparatively stronger in the homogeneous case (Fig. 5b). Differences in the lake-breeze flow caused by roughness are also present southeast of the domain (Fig. 5a).

During the night, the wind intensity is weaker and the turbulence is very small. Therefore, the near-surface flow does not respond to the roughness length variation as it does during daytime. At 0600 LT the roughness effect is not very clear, with the wind field generated by expt 1 (Fig. 6) and expt 2 (homogeneous land use, not shown here) not presenting many differences.

The role of topography can be verified by comparing the wind fields simulated in expt 2 (realistic topography) and expt 3 (flat topography). The lake is present and the land use is assumed to be homogeneous in both simulations. Figures 5b and 5c show that at the end of daytime the horizontal wind field divergence intensity is basically due to the presence of the lake. It is interesting to note that the lake-breeze horizontal extension is larger in the realistic topography cases because of the lake-breeze inland propagation intensification caused by the anabatic flow present in the mountain–valley circulation (Figs. 5a,b). This effect can be better visualized when the lake is removed and the topography is maintained as realistic, as in expt 4 (Fig. 5d). In this case, a weak anabatic flow can be seen causing divergence in the bottom of the valley.

b. Diurnal evolution of temperature and specific humidity

It will be assumed, hereinafter, that the best representation of the Itaipu Lake local circulation for undisturbed synoptic conditions, during a summer period, is given by expt 1 (realistic topography and land use). Therefore, all the results presented and discussed henceforth are based on the numerical results generated by expt 1. The observations used hereinafter are based on the meteorological dataset available from the region (section 2).

The modeled diurnal evolution of the horizontal thermal contrast between the lake and its surrounding land can be seen in Fig. 7a where the air temperature difference between Itaipu Lake and the Itaipu power plant, at the surface and 15 m, is displayed. During daytime, the maximum horizontal thermal contrast induced by the lake occurs around midday, being on the order of -13°C at surface level and around -2°C at 15 m. These values match with the thermal contrast inferred from the observations (Fig. 7b) if it is considered that the observations were carried out at screen height (1.5 m) and that the largest vertical gradients of temperature are confined near to the surface. During daytime, the observed thermal contrast induced by Itaipu Lake at a 1.5-m height is negative, varying from 0° to -1.5°C during the winter/spring months, and between -2° and -3°C during the summer/autumn months.

During nighttime, the modeled horizontal thermal contrast induced by the lake is positive, reaching its largest value, at 0500 LT, of about 7°C at surface and 1°C at 15 m (Fig. 7). These values do not match well with the inferred ones (between 8.5° and 9.5°C; Fig. 7b). The observations and numerical simulations have the right signal but their amplitude discrepancies are large and cannot be explained with the available observations.

c. Diurnal evolution of horizontal wind and horizontal wind divergence

The diurnal evolution of the simulated horizontal wind velocity at Foz do Iguaçu Airport (Figs. 8b and

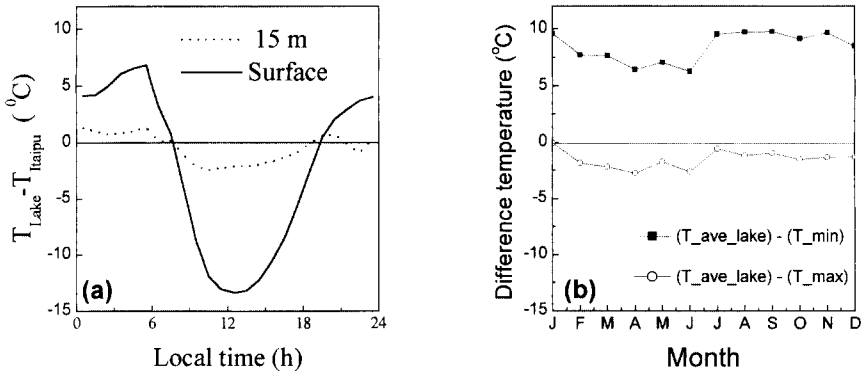

FIG. 7. (a) Model time evolution of the air temperature difference between Itaipu Lake (T_{Lake}) and the Itaipu power plant (T_{Itaipu}). The solid and dotted lines correspond, respectively, to surface and 15-m measurements. (b) Monthly evolution of the observed difference between the monthly averaged daily temperature over Itaipu Lake (T_ave_lake) and the monthly averaged daily temperature max (T_max) (full squared line) and min (T_min) (open circle line) at the Itaipu power plant meteorological station. The observations were carried out at screen height (1.5 m).

9b) demonstrates similarity with the observations, showing that the daytime lake breeze and the nighttime land breeze affect the wind diurnal evolution at this place. The simulated wind amplitude at Itaipu power plant (Figs. 8a and 9a), however, is considerably larger than the observed wind amplitude at the same location. Between 0900 and 1600 LT, the wind vector presents a clockwise rotation at the Itaipu power plant (Fig. 9a) and a counterclockwise rotation at Foz do Iguaçu Airport (Fig. 9b). Between 1600 and 2400 LT the wind vector at the Itaipu power plant rotates counterclockwise, while at Foz do Iguaçu Airport it remains rotating counterclockwise. During daytime the wind rotation pattern is consistent with the lake-breeze circulation system.

The diurnal evolution of the horizontal divergence (Fig. 10), estimated using the wind simulated in grid points corresponding to Foz do Iguaçu Airport and the Itaipu power plant (Fig. 2), matches well with the observed divergence. However, during daytime, the maximum amplitude of the simulated divergence is about twice the observed divergence in the area. On the contrary, nighttime observations indicate a larger convergence.

d. Vertical and horizontal lake-breeze extent

The analysis of the lake-breeze spatial distribution—carried out in terms of its inland propagation, intensity, and vertical depth—was performed investigating the wind field cross sections in the vertical plane, aligned to the latitude of the Itaipu power plant (Fig. 2a). Along

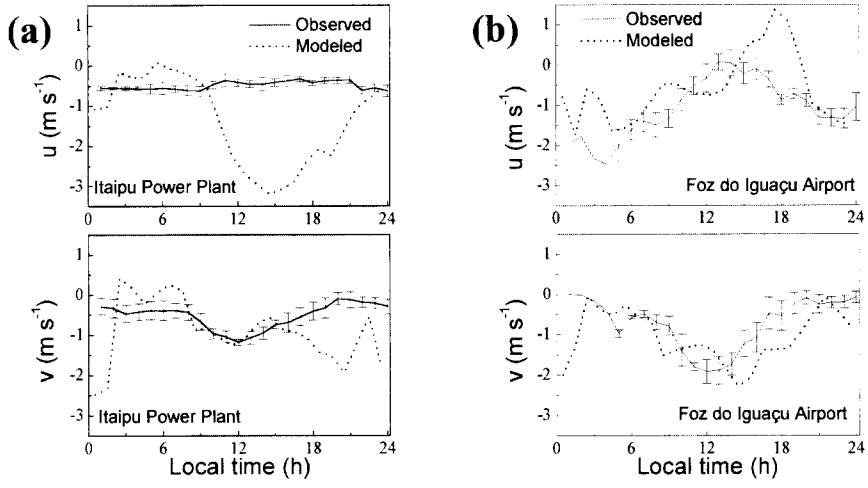

FIG. 8. Temporal evolution of the (top) zonal and (bottom) meridional wind components at (a) the Itaipu power plant and (b) Foz do Iguaçu Airport. The dotted lines represent the modeled values and the continuous lines are the observed values. The vertical bars correspond to statistical error.

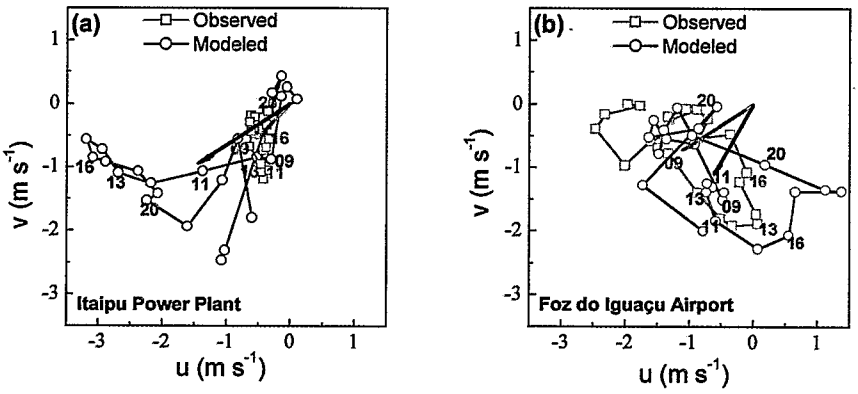

FIG. 9. Hodograph for the temporal evolution of the winds at (a) the Itaipu power plant and (b) Foz do Iguaçu Airport. The modeled hodograph (black) corresponds to hourly winds, and the observed hodograph (red) corresponds to the hourly monthly averaged winds. The numbers indicate LT, and the arrows correspond to the daily averaged wind.

this latitude the lake is approximately 10 km wide and the land use is predominantly pasture (smoother) on the western side of the lake and agriculture (rougher) on the eastern side (Fig. 2b). On the eastern side of the lake, there is a lake branch, about 4 km wide, connected to the main water body. Between the main lake and this branch there is about 2 km of land covered by pasture. In this latitude, the lake margins are located between $x = 44$ km and $x = 64$ km and are shown as vertical lines in Figs. 11–15.

After midday, the circulation around the lake vicinities becomes a defined lake-breeze circulation, presenting a clear horizontal divergence in the zonal (x) direction over the lake area (Figs. 11a–c). At 1500 LT (Fig. 11a) the lake-breeze circulation in the zonal direction reaches -2.5 m s^{-1} on the western side of the lake at $x = 20$ km and 2.0 m s^{-1} on the eastern side at $x = 68$ km and $x = 74$ km. The existence of two cores on the eastern side of the lake is related to the lake branch presence. At 1800 LT (Fig. 11b) the lake breeze reaches its maximum intensity and horizontal extension, with -3.5 m s^{-1} on the western side of the lake at $x = 10$ km and 2 m s^{-1} on the eastern side of the lake at $x = 75$ km. At 2100 LT (Fig. 11c) most of the domain is under negative zonal component flow. The vertical extent of the lake breeze can be inferred from the vertical extent of the direct circulation; between 1500 (Fig. 11a) and 1800 LT (Fig. 11b) it reaches about 1500 m on both sides of the lake. During this period the lake-breeze countercurrent is confined to the layer between 1500 and 3000 m (Figs. 11a,b). At 0600 LT the flow has a very small component in the zonal direction (Fig. 11d).

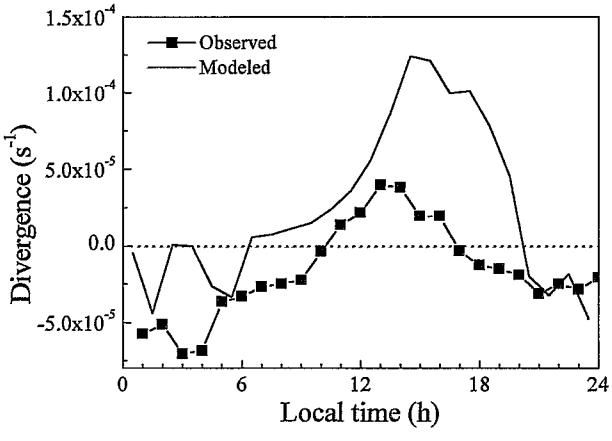

FIG. 10. Time evolution of the modeled (continuous line) and observed (line and solid square) horizontal wind divergence from the winds at the Itaipu power plant and Foz do Iguaçu Airport. The observed divergence was estimated from the monthly averaged winds.

On the eastern side of the lake at 1500 LT the meridional wind component (Fig. 12a) indicates the presence of two negative cores near the surface—one over the lake and another over its branch—that seem to be associated with the channeling effects caused by the stable stratified surface layer over the lake. Over land, the lake-breeze circulation induces a positive core on the eastern side of the lake at $x = 90$ km and on the western side at $x = 5$ km. At the end of the night (Fig. 12b) the horizontal flow is basically meridional once, at this hour, the wind zonal component is very weak over the entire domain (Fig. 11d).

As mentioned above, the lake-breeze front is characterized by convergence and vertical motion. Following the inland propagation of this front between 1200 (not shown here) and 1800 LT it can be found that the lake breeze in the Itaipu power plant latitude propagates inland at approximately 5.1 km h^{-1} (average over both sides). Numerical simulations with 50-km-wide lakes have shown propagation speeds of 5 (Neumann and Mahrer 1975) and 10 km h^{-1} (Physick 1976). When compared with the larger lakes, the Itaipu Lake breeze front propagates inland faster because of the topographic mountain–valley circulation, which contributes to the inland propagation. Despite other effects that can influence the inland lake-breeze propagation, such as the

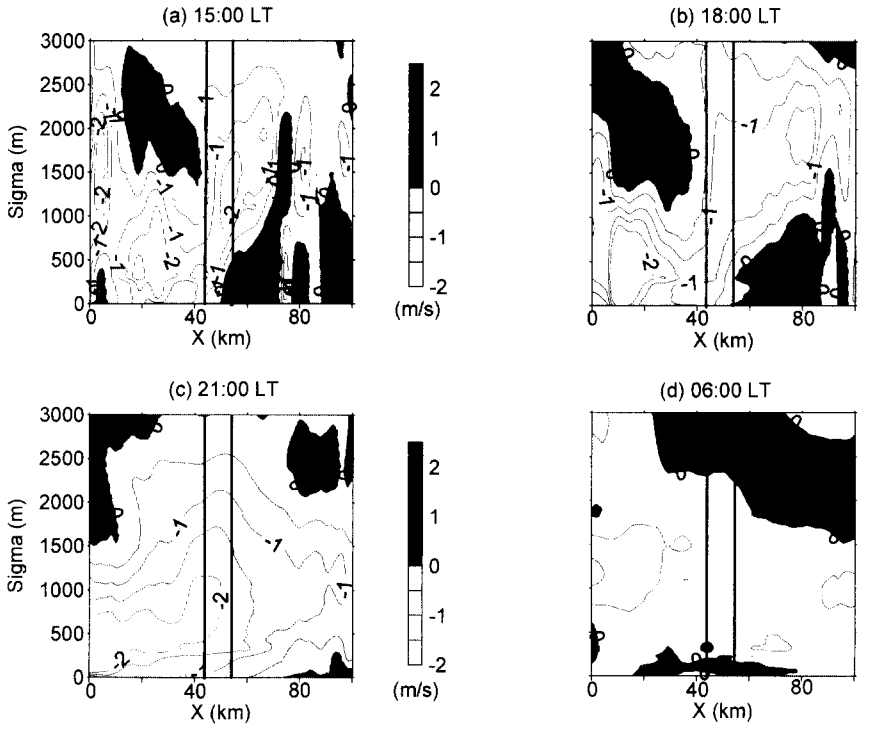

FIG. 11. Cross section along the Itaipu power plant latitude for the zonal component of wind velocity (m s^{-1}) at (a) 1500, (b) 1800, (c) 2100, and (d) 0600 LT. The vertical lines indicate the lake position.

effects caused by the land use, the largest inland propagation velocity was obtained with the most realistic experiment, as can be seen by comparing the lake-breeze fronts in Figs. 5a–c.

e. *Impact of the lake-breeze circulation on the local PBL*

The spatial distributions of potential temperature (Fig. 13) and specific humidity (Fig. 14), at 1500 and 1800 LT, reveal the impact caused by Itaipu Lake on the local PBL. At 1500 LT there is a very well developed mixed layer with a potential temperature of 309 K and a vertical extension varying from 1900 m in the western part of the domain to about 1500 m in the remainder of the domain, except over the lake (Fig. 13a). There is also a very convective surface layer with superadiabatic vertical gradients concentrated in the first 250 m. Over the lake, the PBL is stably stratified and much cooler than over land. The horizontal thermal contrast, caused by the presence of the lake, can be noticed up to 1000 m. At 1800 LT, the superadiabatic vertical gradients have subsided, and the colder area around the lake indicates how wide the cooling induced by the lake in the PBL was (Fig. 13b). At this time, the mixed-layer vertical extension gets smaller, reaching over the eastern side of

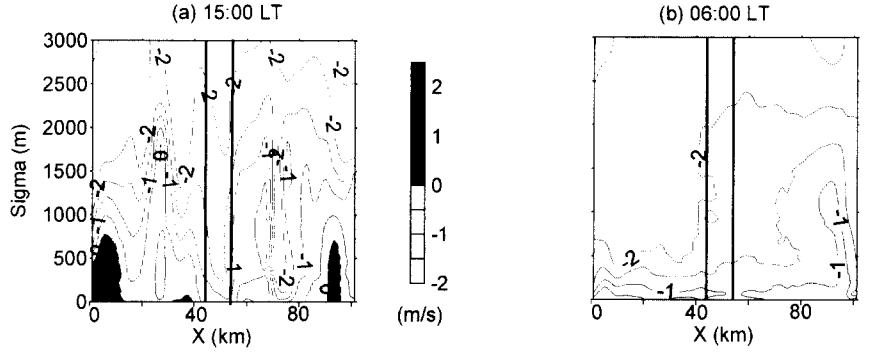

FIG. 12. Same as in Fig. 11 but for the meridional component of wind velocity (m s^{-1}) at (a) 1500 and (b) 0600 LT. The vertical lines indicate the lake position.

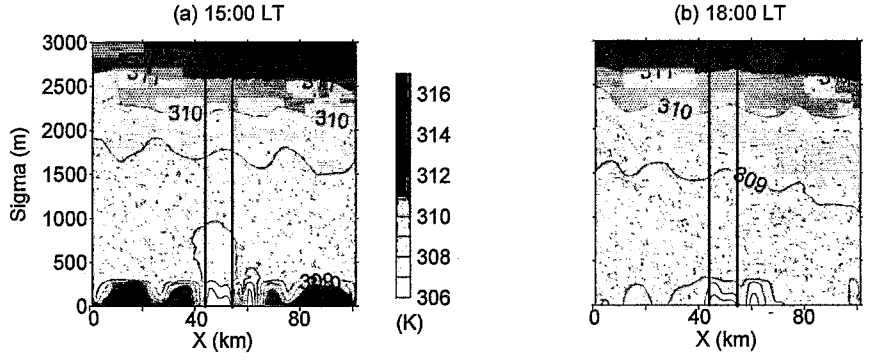

FIG. 13. Same as in Fig. 11 but for potential temperature (K) at (a) 1500 and (b) 1800 LT. The vertical lines indicate the lake position.

the lake about 1000 m. The shrinking of the mixed-layer extension is caused by the intensification of the radiation cooling of the atmosphere at the end of day.

The specific humidity follows a similar pattern. At 1500 LT, a 1500-m-high mixed layer with specific humidity on the order of 11 g kg^{-1} is present over land (Fig. 14a). At 1800 LT, the layer with specific humidity equal to 11 g kg^{-1} can be observed up to 2000 m over land (Fig. 14b). At both times, over the lake the moisture is larger than over the land, in the first 250 m; above this level, the specific humidity over the lake is always smaller than over the land. The horizontal contrast between the lake and the land, above 250 m, reaches as much as -4 g kg^{-1} at 1500 LT (Fig. 14a) and -5 g kg^{-1} at 1800 LT (Fig. 14b). The intense moisture contrast is due to the subsidence of drier air over the lake and the presence of intense turbulent PBL mixing over land, generated during the maximum solar heating period of the day. In the first 250 m, the advection of moisture has a minor role in the spatial distribution of specific humidity in comparison with the vertical divergence of the vertical turbulent flux.

The PBL height, at 1500 LT, can be better visualized by the TKE spatial distribution at 1500 LT (Fig. 15). The TKE over the lake is very small, near zero. Over land areas the TKE reaches a maximum of 2.3 m^2 s^{-2}. During nighttime, as a result of the low wind intensity close to the surface, the turbulence intensity is very small (not shown here). It is interesting to observe the good matching between the spatial patterns of potential temperature (Fig. 13a), the surface layer vertical gradient of specific humidity (Fig. 14a), and the TKE (Fig. 15). These results are consistent and show that during daytime the lake-breeze circulation, induced by the lake, has a strong effect on the PBL area around the lake.

5. Discussion and conclusions

The lake-breeze circulation over the Itaipu Lake area was numerically investigated using a mesoscale model called NH-TVM. The numerical simulations included realistic topography and land use information in a 100 km × 180 km area around the lake. Initial and boundary conditions were set up to reproduce a typical undisturbed condition during summer in the area.

Four different numerical experiments were performed to investigate the role played by topography, land use, and lake-breeze circulations in the Itaipu area. Expt 1 included realistic topography and land use with the lake presence; expt 2 included realistic topography and homogeneous land use with the lake presence; expt 3 utilized level topography and homogeneous land use with

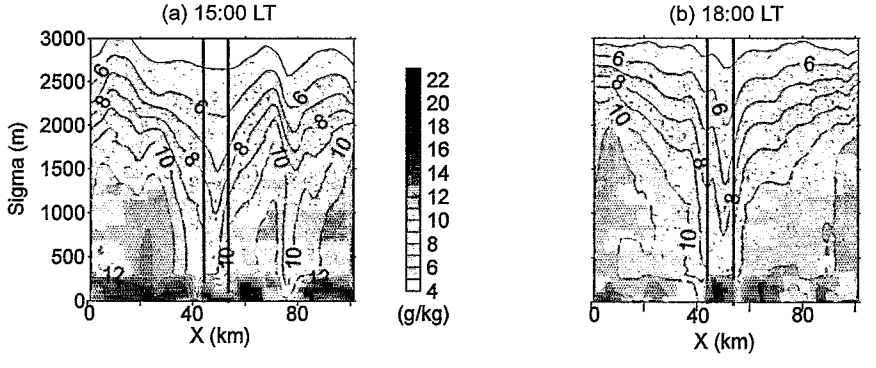

FIG. 14. Cross section along the Itaipu power plant latitude for specific humidity (g kg^{-1}) at (a) 1500 and (b) 1800 LT. The vertical lines indicate the lake position.

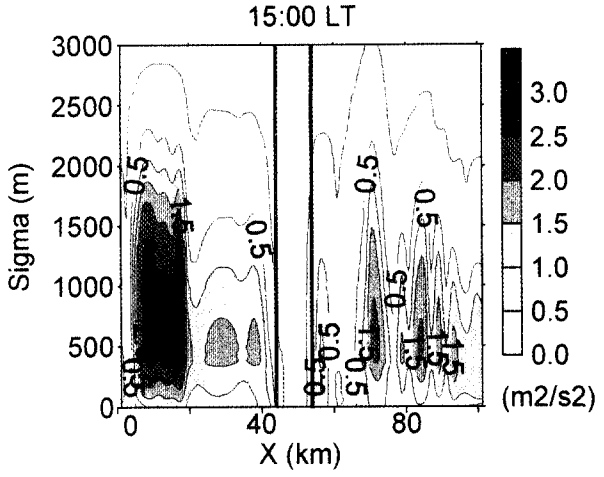

FIG. 15. Cross section along the Itaipu power plant latitude for turbulent kinetic energy ($m^2 s^{-2}$) at 1500 LT. The vertical lines indicate the lake position.

the lake presence; expt 4 assumed realistic topography and homogeneous land use without the lake presence.

The first conclusion is that Itaipu Lake (7.5 km wide and 170 km long) was able to generate and sustain a lake breeze, which is formed around 1200 LT and dies out around 2100 LT. Regardless of the land use and topography, the presence of Itaipu Lake is the main reason for the existence of the lake breeze in the Itaipu valley area during daytime. The numerical results indicated that the convergence zone follows the lake contour, even in its complex part where the lake branches out. When the realistic topography is considered in the model, the circulation induced by the lake is much stronger and more defined than the circulation obtained when the lake is removed. The lake breeze becomes visible around 1200 LT and reaches its maximum intensity and size approximately at 1800 LT. The negative horizontal thermal contrast associated with the presence of the lake is the main cause of the lake breeze. The maximum horizontal differential heating between land and lake occurs around 1500 LT (13 K at the surface and 2 K at 15 m). At this time, the vertical extent of the direct circulation is on the order of 1500 m, the maximum vertical motion is approximately 60 cm s^{-1}, and the lake-breeze intensity is approximately 2.5 m s^{-1}. At 1800 LT the lake breeze reaches its maximum intensity (~3.5 m s^{-1}) and horizontal extension (~50 km).

It was found that the land use effect is important in the spatial distribution of the lake-breeze circulation in the region of Itaipu Lake. The results indicated that the lake breeze is more intense and spreads over a larger area when the realistic land use is substituted by homogeneous land use. This effect is basically due to the roughness length; the lake breeze can be retarded in the regions covered by forest (eastern side), inducing horizontal convergence and sustaining stronger vertical motion. The topography contributes to modulation of the lake-breeze intensity. The valley–mountain thermal contrast seems to be intense and acting over a horizontal area large enough to contribute to the horizontal divergence over the lake area by an anabatic circulation. Therefore, the lake breeze is stronger in the presence of topography. During nighttime there is an incipient convergence over the investigated area that seems to be associated with the positive thermal contrast. This effect becomes more visible at 0600 LT when the thermal contrast reaches its maximum. The existence of a convergence zone over the bottom of the valley, when the lake is removed, indicates that the katabatic circulation may be contributing to the observed convergence pattern during nighttime when the lake is present.

The characteristics of the lake breeze generated by the numerical experiments are consistent with the observations available in the area. The discrepancies found between observed and modeled results can be due to the fact that the comparison is between modeled typical cases and monthly averaged observations. It is very difficult for the model to reproduce averaged circulations. The study performed here, however, has its validity restricted to the summer conditions in the Itaipu region. The agriculturally active areas can change seasonally and, therefore, one could expect to find a different circulation pattern during the winter period. The different large-scale circulation and the seasonal variation of soil water content could also affect the lake-breeze circulation over the region. According to Shen (1998), the stronger effect would be related to the seasonal variation of the soil water content. A deeper inland lake-breeze penetration could also be expected because the forest, in the western side of the region, is progressively being replaced by agricultural areas. The next step will be the investigation of the lake-breeze circulation over Itaipu during winter conditions.

Acknowledgments. The authors thank the CNPq and FAPESP for sponsoring this research.

REFERENCES

Bornstein, R. D., 1975: The two-dimensional URBMET urban boundary layer model. *J. Appl. Meteor.*, **14,** 1459–1477.

——, P. Thunis, P. Grossi, and G. Schayes, 1996: Topographic vorticity-mode mesoscale-β (TVM) model. Part II: Evaluation. *J. Appl. Meteor.*, **35,** 1824–1834.

Colella, P., and P. R. Woodward, 1984: The piecewise parabolic method (PPM) for gas-dynamical simulations. *J. Comput. Phys.*, **54,** 174–201.

Durran, D. R., 1990: Mountain waves and downslope winds. *Atmospheric Processes over Complex Terrain, Meteor. Monogr.*, No. 45, Amer. Meteor. Soc., 59–81.

Garratt, J. R., 1992: *The Atmospheric Boundary Layer.* Cambridge University Press, 316 pp.

Martin, F., S. N. Crespí, and M. Palacios, 2001a: Simulations of mesoscale circulations in the center of the Iberian Peninsula for thermal low pressure conditions. Part I: Evaluation of the topography vorticity-mode mesoscale model. *J. Appl. Meteor.*, **40,** 880–904.

——, M. Palacios, and S. N. Crespí, 2001b: Simulations of mesoscale

circulations in the center of the Iberian Peninsula for thermal low pressure conditions. Part II: Air-parcel transport patterns. *J. Appl. Meteor.*, **40,** 905–914.

Neumann, J., and Y. Mahrer, 1975: A theoretical study of the lake and land breeze of circular lakes. *Mon. Wea. Rev.,* **103,** 474–485.

Physick, W., 1976: A numerical model of the sea-breeze phenomenon over a lake or gulf. *J. Atmos. Sci.*, **33,** 2107–2135.

Pielke, R. A., and M. Segal, 1986: Mesoscale circulations forced by differential terrain heating. *Mesoscale Meteorology and Forecasting,* P. S. Ray, Ed., Amer. Meteor. Soc., 516–548.

Ratisbona, L. R., 1976: The Climate of Brazil. *Climates of Central and South America*, Vol. 12, *World Survey of Climatology,* W. Schwerdtfeger and H. E. Landsberg, Eds., Elsevier, 219–293.

Schayes, G., and P. Thunis, 1990: The three-dimensional mesoscale model in vorticity mode (TVM). Contribution 60, Institut d'Astronomie et de Geophysique Georges Lemaitre, Université Catholique de Louvain, Louvein-la-Neuve, Belgium, 42 pp. [Available from Chemin du Cyclotron, 2, 1348 Louvain-La-Neuve, Belgium.]

——, ——, and R. Bornstein, 1996: Topographic vorticity mesoscale-β (TVM) model. Part I: Formulation. *J. Appl. Meteor.*, **35,** 1815–1823.

Segal, M., M. Leuthold, R. W. Arritt, C. Anderson, and J. Shen, 1997: Small lake daytime breezes: Some observational and conceptual evaluations. *Bull. Amer. Meteor. Soc.,* **78,** 1135–1147.

Sellers, W. D., 1965: *Physical Climatology.* University of Chicago Press, 272 pp.

Shen, J., 1998: Numerical modeling of the effects of vegetation and environmental conditions on the lake breeze. *Bound.-Layer Meteor.,* **87,** 481–498.

Stivari, S. M., 1999: Um estudo da brisa lacustre do Lago de Itaipu. Ph.D. thesis, Dept. of Atmospheric Sciences, University of São Paulo, Brazil, 126 pp. [Available from Rua do Matão, 1226, São Paulo, SP 05508.900, Brazil.]

Stull, R. B., 1988: *An Introduction to Boundary Layer Meteorology.* Kluwer Academic, 666 pp.

Thunis, P., and A. Clappier, 2000: Formulation and evaluation of a nonhydrostatic mesoscale vorticity model (TVM). *Mon. Wea. Rev.,* **128,** 3236–3251.